ELSEVIER

www.elsevier.nl/locate/jorganchem

Journal of Organometallic Chemistry 584 (1999) 190–196

Journal of Organometallic Chemistry

Photochemical generation of a novel (O, N′, N″) coordinated iron(II) complex [Fe(FT–py)$_2$] from a ferrocenoyl-functionalized thiourea ligand: *N*-ferrocenylcarbonyl-*N*′-(2-pyridyl)thiourea (HFT–py): crystal and molecular structures of HFT–py and [Fe(FT–py)$_2$]

De-Ji Che [a,*], Gang Li [a], Xiao-Lan Yao [a], Qiang-Jin Wu [b], Wen-Ling Wang [a], Yu Zhu [a]

[a] *Department of Chemistry, Zhengzhou University, Henan 450052, People's Republic of China*

[b] *State Key Laboratory of Structural Chemistry of matter, Chinese Academy of Sciences, Fuzhou, Fujian 350002, People's Republic of China*

Received 3 December 1998; received in revised form 2 March 1999

Abstract

Photolysis of deoxygenated acetonitrile solution of a ferrocenoyl-functionalized thiourea ligand, *N*-ferrocenylcarbonyl-*N*′-(2-pyridyl)thiourea (HFT–py) with visible light leads to the formation of a novel (O, N′, N″) coordinated iron(II) complex [Fe(FT–py)$_2$], in which two deprotonated ligands (FT–py$^-$) are bound to one iron(II) centre through a carbonyl oxygen O, deprotonated thioamidic (–C(S)–N′H–) nitrogen N′ and pyridyl nitrogen N″ atoms to form a distorted octahedral complex. In the photolysis process, the photochemical activation plays an important role in the deprotonation of the intramolecular hydrogen bond (O···H–N′) to provide both O, N′ donor sites. The molecular structures of the ligand and its photoproduct were determined by X-ray diffraction, which unequivocally confirmed the photochemical behaviour and the coordination feature.

Keywords: Ferrocenoyl; Photolysis; Charge transfer; Proton transfer; Acylthiourea

1. Introduction

Ferrocene is well known to be photo-inert. However, we [1,2] and others [3,4] have demonstrated that the ferrocenoyl-containing compounds exhibit remarkable photo-activity due to photo-induced charge transfer from ferrocenyl to the electron-drawing carbonyl group, leading to the cleavage of the bonds between iron(II) and acylcyclopentadienyl rings in the ferrocenoyl. Therefore, if such a group as a photo-active centre is incorporated into ligands, they may behave as photoresponsive complex systems, and hence have potential as photosensitive materials, just as ferrocene-containing ligands, in which the ferrocene acts as a redox-active centre, have been shown to have useful properties for new materials and have attracted considerable attention in recent years [5–8].

With the aim of elucidating the photo-activity of this class of ligands, we have recently studied the photoreaction of a ferrocenoyl-functionalized thiourea ligand, *N*-ferrocenylcarbonyl-*N*′-(2-pyridyl)thiourea (HFT–py), Fc–C(O)–NH–C(S)–N′H–(C_5H_4N″), and structurally characterized the ligand (HFT–py) and its photoproduct [Fe(FT–py)$_2$] to reveal the photochemical behaviour and the unusual coordination feature.

2. Experimental

2.1. Materials and analytical equipment

All the chemicals used in this study were of analytical grade without further purification. All the solvents were dried and distilled prior to use [9]. Infrared spectra were recorded on a Shimadzu IR-435 instrument using KBr pellets in the 400–4000 cm^{-1} region. Elemental analy-

* Corresponding author. Fax: +86-371-7970475.

0022-328X/99/$ - see front matter
PII: S0022-328X(99)00138-2

ses were carried out on a MOD 1106 analyzer. UV–vis spectra were taken on a Hitachi 220A spectrophotometer with 1 cm matching quartz cell.

2.2. Synthesis of HFT–py

HFT–py was prepared using a similar procedure described in the literature [10] by the reaction of ferrocenoyl chloride with KSCN in anhydrous acetone to produce ferrocenoyl *iso*thiocyanate followed by condensation with 2-aminopyridine. The product was recrystallized from acetone and characterized by elemental analysis. Yield: ca. 82%. Anal. Calc. for ($C_{17}H_{15}FeN_3OS$): C, 55.89; H, 4.11; N, 11.51%. Found: C, 55.86; H, 4.17; N, 11.66%. IR data were presented in Table 7.

2.3. Photolysis of HFT–py

A solution of HFT–py (40 mg) in 10 cm^3 of CH_3CN was deoxygenated prior to photolysis and irradiated at 0°C in an ice bath for 1 h under visible light from a 200 W xenon lamp. After the irradiation, the solution was put aside overnight. One of the photoproducts, [Fe(FT–py)$_2$] was crystallized from the solution, which afforded the analytical sample and single crystals suitable for X-ray crystallography. Yield: ca. 12%, m.p. 194°C (dec.). Anal. Calc. for ($Fe(C_{17}H_{14}FeN_3OS)_2$): C, 52.07; H, 3.57: N, 10.72%. Found: C, 51.79; H, 3.71; N, 10.73%. IR data were presented in Table 7. Mass spectrum: the molecular ion peak was not detected, probably due to its ready dissociation; the fragmentary mass data are deposited in the supplementary material.

2.4. Crystallography

2.4.1. HFT–py

A deep-red prismatic crystal of HFT–py with dimensions of $0.80 \times 0.30 \times 0.20$ mm was mounted on a Rigaku RAXIS-IV imaging plate area detector with graphite monochromated Mo–K_α radiation ($\lambda = 0.71$ Å) for unit-cell determination and data collection. Summaries of the crystallographic data, structure solution and refinement are given in Table 1.

A total of 23 3.00° oscillation frames with an exposure time of 15.0 min per frame were used. The structure was solved by direct methods and expanded using Fourier techniques. The data were corrected for Lorentz and polarization effects. The non-hydrogen atoms were refined anisotropically and hydrogen atoms were included but not refined. The teXsan crystallographic software package of Molecular Structure Corporation [11] was used for all calculations.

The principal bond distances and angles, the least-squares planes and dihedral angles are given in Tables 2 and 3, respectively.

Table 1
Crystal data and experimental parameters [a]

	HFT–py	[Fe(FT–py)$_2$]
Formula	$C_{17}H_{15}FeN_3OS$	$C_{34}H_{28}Fe_3N_6O_2S_2$
Formula weight	364.85	783.55
Crystal dimensions (mm)	$0.8 \times 0.3 \times 0.2$	$0.2 \times 0.5 \times 0.8$
Crystal color	Deep red, prismatic	Dark red
Crystal system	Orthorhombic	Monoclinic
Space group	$Pca2_1$ (#29)	$C2/c$ (#15)
a (Å)	14.657(4)	22.09(1)
b (Å)	19.096(4)	10.756(4)
c (Å)	11.511(3)	27.615(6)
β (°)		94.86(3)
V (Å^3)	3221.9	6357(5)
Z	8	8
Diffractometer	Rigaku RAXIS-IV	Rigaku AFc5R
$D_{calc.}$ (g cm^{-3})	1.506	1.594
μ (Mo–K_α) (cm^{-1})	10.71	14.78
$2\theta_{max}$ (°)	55.0	25
Scan mode		$\omega - 2\theta$
Scan width (°)		$1.092 + 0.35 \tan(\theta)$
Data collected (h, k, l)	h 0–18	h 0–26
	k 0–24	k 0–18
	l 0–14	l −33–33
No. of reflections measured	3300	6109
No. of observed refills ($I \geq 3\sigma(I)$)	2620	4456
No. of refined parameters	416	424
R (%)	3.2	4.3
R_w (%)	4.3	5.9
Goodness-of-fit	1.20	1.59
$\Delta\rho$ (max, min) (e Å^{-3})	0.24, −0.42	0.380, −0.046

[a] $R = \Sigma(|F_o| - |F_c|)/\Sigma|F_o|$; $R_w = [\Sigma W(|F_o| - |F_c|)^2/wF_o^2]^{1/2}$.

2.4.2. [Fe(FT–py)$_2$]

A dark-red–black crystal of [Fe(FT–py)$_2$] with dimensions of $0.2 \times 0.5 \times 0.8$ mm was mounted on a Rigaku-AFc5R diffractometer to perform X-ray diffraction work using graphite monochromatized Mo–K_α radiation ($\lambda = 0.71069$ Å). The unit-cell parameters were determination and refined by a least-squares treatment of the setting angles of 20 automatically centred

Table 2
Principal bond distances (Å) and angles (°) for HFT–py

Bond length (Å)			
S(1)–C(1)	1.613(9)	S(1)–C(1)–N(2)	129.2(7)
O(1)–C(2)	1.23(1)	S(1)–C(1)–N(3)	118.7(6)
N(2)–C(1)	1.41(1)	N(2)–C(1)–N(3)	112.0(7)
N(2)–C(11)	1.36(1)	O(1)–C(2)–N(3)	119.6(9)
N(3)–C(1)	1.42(1)	O(1)–C(2)–C(51)	125.9(9)
N(3)–C(2)	1.39(1)	N(3)–C(2)–C(51)	114.5(8)
C(2)–C(51)	1.48(1)	C(11)–N(2)–C(1)	124.3(8)
		N(5)–C(11)–N(2)	116.7(8)
Hydrogen bonding and bond angle (°)			
N(2)···O(1)	2.64(1)	N(2)–H···O(1)	135.63
N(2)–H	0.939	O(1)···H	1.889

Table 3
Least-squares planes and dihedral angles (°) for HFT–py

Plane 1		Plane 2		Plane 3	
Atoms	Distance	Atoms	Distance	Atoms	Distance
N(2)	−0.09(1)	N(5)	−0.01(2)	C(51)	−0.01(1)
C(1)	−0.05(1)	C(11)	0.02(2)	C(52)	−0.01(1)
S(1)	0.008(5)	C(12)	−0.01(2)	C(53)	−0.02(1)
N(3)	−0.133(10)	C(13)	−0.02(2)	C(54)	0.03(1)
C(2)	0.00(1)	C(14)	0.03(2)	C(55)	−0.02(1)
O(1)	0.15(1)	C(15)	−0.01(2)		
Dihedral angle (°) between planes					
1/2	37.60		2/3	27.24	

reflections ($7° < \theta < 10°$). The intensity data were collected by using $\omega - 2\theta$ scan mode in the range $25° \geq \theta \geq 1°$. A variable scan speed was used. Total of 6286 reflections were measured and corrected for LP effects and for the absorption using the ψ scan technique. After equivalent reflection intensities were averaged. A total of 6109 independent intensities data were obtained. Of which 4456 with intensities $I \geq 3\sigma(I)$ were used in the structure solution and refinements. The structure was solved by a combination of direct method (MITHRIL) and difference Fourier syntheses. All nonhydrogen atoms were refined with anisotropic thermal parameter. The hydrogen positions were located in the difference Fourier maps and included in the calculations without further refinement. The pertinent crystallographic data and experiment details are listed in Table 1. All calculations were carried out on a MICROVAXII computer using the teXsan crystallographic software package of the Molecular Structure Corporation [11]. The principal bond distances and angles, the least-squares planes and dihedral angles are shown in Tables 4 and 5, respectively.

3. Results and discussion

3.1. Molecular structure of the ligand, HFT–py

The structure of HFT–py is very similar to those reported by Wang [12] and Yuan [13] for analogous acylthioureas: *N*-(ferrocenylcarbonyl)-*N′*-naphthylthiourea and 1,1′-bis(*N*-formyl-*N′*-*p*-chlorophenylthiourea)ferrocene. These molecules exhibit two features: first, an intramolecular hydrogen bond (O…H—N′) is formed between carbonyl oxygen atom and the hydrogen atom on N′ in the planar –C(O)–NH–C(S)–N′H– moiety (I). Secondly, both carbonyl and thiocarbonyl groups occupy anti-positions to each other in the plane I, which is favourable to establish the observed hydrogen bonding, but the pyridyl N″ atom is in *syn*-positions with the carbonyl oxygen atom, the pyridyl ring has a dihedral angle of ca. 40° with the plane I. The molecular structure of HFT–py is shown in Fig. 1.

3.2. Molecular structure of the photoproduct [Fe(FT–py)$_2$]

A drawing of the complex with the atomic numbering scheme is shown in Fig. 2 and selected bond lengths and angles in Table 4. The structure consists of discrete neutral molecules [Fe(FT–py)$_2$]; in each molecule both deprotonated ligands (FT–py$^-$) are bound to one iron(II) centre through carbonyl oxygen O, deprotonated thioamidic (–C(S)–N′–) nitrogen N′ and pyridyl nitrogen N″ atoms to give a distorted octahedral Fe(II) complex with a $FeO_2N'_2N''_2$ kernel, where the coordinate bond distances (Fe–N, Fe–O) lie in the range

Table 4
Principal bond distances (Å) and angles (°) for [Fe(FT–py)$_2$]

Fe(3)–O(1)	2.050(3)	O(2)–C(4)	1.228(5)
Fe(3)–O(2)	2.082(3)	N(1)–C(21)	1.393(5)
Fe(3)–N(1)	2.091(3)	N(6)–C(21)	1.343(5)
Fe(3)–N(2)	2.118(3)	N(2)–C(11)	1.400(5)
Fe(3)–N(5)	2.179(4)	N(5)–C(11)	1.351(5)
Fe(3)–N(6)	2.242(4)	N(2)–C(1)	1.314(5)
N(1)–C(3)	1.309(5)	N(3)–C(1)	1.421(5)
N(4)–C(3)	1.420(5)	O(1)–C(2)	1.240(5)
N(4)–C(4)	1.375(5)	S(1)–C(1)	1.678(4)
N(3)–C(2)	1.361(5)	S(2)–C(3)	1.680(4)
O(1)–Fe(3)–O(2)	97.3(1)	N(1)–Fe(3)–N(2)	168.4(1)
O(1)–Fe(3)–N(1)	103.3(1)	N(1)–Fe(3)–N(5)	113.1(1)
O(1)–Fe(3)–N(2)	81.1(1)	N(1)–Fe(3)–N(6)	61.1(1)
O(1)–Fe(3)–N(5)	143.1(1)	N(2)–Fe(3)–N(5)	62.0(1)
O(1)–Fe(3)–N(6)	96.4(1)	N(2)–Fe(3)–N(6)	108.0(1)
O(2)–Fe(3)–N(1)	82.4(1)	N(5)–Fe(3)–N(6)	96.1(1)
O(2)–Fe(3)–N(2)	107.9(1)		
O(2)–Fe(3)–N(5)	93.1(1)		
O(2)–Fe(3)–N(6)	143.1(1)		

Table 5
Least-squares planes and dihedral angle (°) for [Fe(FT–py)$_2$]

Plane 1		Plane 2	
Atoms	distance	Atoms	distance
O(2)	−0.1111	O(1)	−0.1128
C(4)	−0.0288	C(2)	0.0541
N(4)	0.0664	N(3)	0.0854
C(3)	0.1765	C(1)	0.0542
N(1)	−0.0216	N(2)	−0.0182
N(6)	0.1323	N(5)	0.0934
C(21)	−0.0146	C(11)	−0.0278
C(22)	−0.2111	C(12)	−0.1306
C(23)	−0.2055	C(13)	−0.1034
C(24)	−0.0216	C(14)	0.0268
C(25)	0.1481	C(15)	0.1277
Additional atoms		Additional atoms	
Fe(3)	0.1819	Fe(3)	0.0313
S(2)	0.5825	S(1)	0.1482
C(31)	−0.0351	C(51)	0.2125
H(02)	0.0558	H(01)	0.2232
Dihedral angles (°) between planes 1/2			90.82

2.05–2.42 Å, and the coordinate bond angles deviate considerably from the regular octahedral geometry (Table 4). The thione (=S) sulfur atom does not participate in the coordination, because it extends to the reverse direction with the carbonyl (C=O) and pyridyl groups. Each chelating (–C(O)–NH–C(S)–N′–(C_5H_4N'')–) moiety is almost planar (Table 5). The dihedral angle between both chelating planes is near vertical (90.82°).

It should be pointed out that the coordination mode in the photoproduct [Fe(FT–py)$_2$], as mentioned above, is apparently different from those in conventional *N*-acylthiourea coordinate compounds. Therefore, a structural comparison was made among them (Table 6). It is apparent that most of the acylthiourea ligands coordinate to the metal ions bidentately via oxygen and sulfur donor sites, exhibiting square-planar (such as nos. 1–5 in Table 6), tetrahedral or octahedral coordination geometry (nos. 7–9), and a few of them coordinate monodentately through sulfur donor only, displaying a linear coordination (no. 10). But today, very little is known about the coordination with O, N′, N″ sites as in the photopoduct, [Fe(FT–py)$_2$]. Of particular interest to us is Bourne's works about the structure of *cis*-bis(*N*–benzoyl-*N*′-propylthiourea) dichloroplatinum(II) (no. 6) in which the two ligand molecules bind to Pt(II) via sulfur atoms only, the carbonyl oxygen atom being locked into a ring by a N–H···O hydrogen bond. However, our result was contrary to that. In [Fe(FT–py)$_2$], the carbonyl oxygen and thioamide N′ donors participating in the coordination were not locked by the hydrogen bond N–H···O in the ligand (Fig. 1). Therefore, it is reasonable to postulate that the photochemical activation may play an important role in deprotonation of the hydrogen bond to provide both O and N′ donor sites for coordination. We have attempted to prepare [Fe(FT–py)$_2$] directly through the reaction of iron(II)chloride with HFT–py beyond irradiation, but were unsuccessful. In addition, each of the chelating moieties consist of three rings, one heterocyclic and two chelates; the presence of the tricyclic ring system gives a planar structure around the metal which contributes to the stability of the iron(II) state [14].

3.3. UV/vis spectral changes upon irradiation

The UV–vis spectrum of HFT–py prior to irradiation, shown in Fig. 3(a), exhibits three moderately

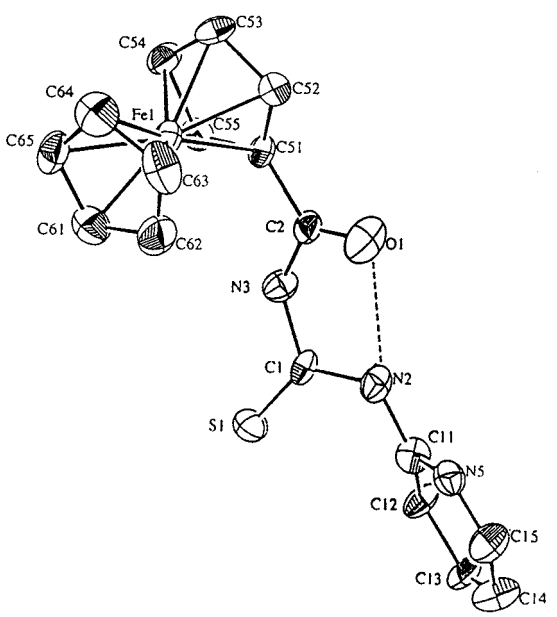

Fig. 1. An ORTEP diagram of HFT–py, showing the atomic-numbering (hydrogen atoms are omitted for clarity).

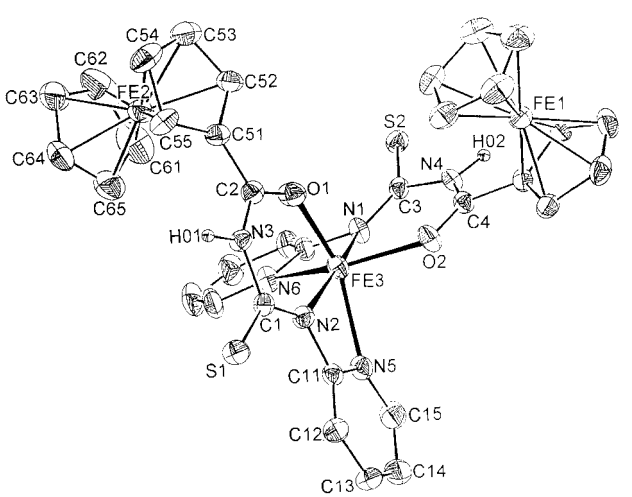

Fig. 2. An ORTEP diagram of [Fe(FT–py)$_2$], showing the atomic-numbering (hydrogen atoms are omitted for clarity).

Table 6
Some structural comparisons for transition-metal complexes of substituted acylthioureasss [a]

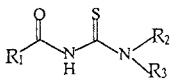

No.	R1	R2	R3	Central ion	Coordination atom	Coordination geometry	Ref.
1	Fc [b]	Et [c]	Et	Ni(II)	O, S	*Cis*-square planar	[20]
2	Ph [d]	Et	Et	Ni(II), Pd(II)	O, S	*Cis* -square planar	[21,22]
3	Ph	Butyl	Butyl	Pt(II)	O, S	*Cis* -square planar	[23]
4	Cl–Ph	Et	Et	Ni(II)	O, S	*Cis* -square planar	[24]
5	Naph [e]	Butyl	Butyl	Pt(II)	O, S	*Trans*-square Planar	[26]
6	Ph	Propyl	H	Pt(II)	S, (Cl)	*Cis* -square planar	[25]
7	Ph	Et	Et	Cu(II)	O, S	Tetrahedral	[27]
8	Ph	Et	Et	Ag(I)	O, (HS)	Tetrahedral	[28]
9	Ph	Et	Et	Ru(III), Rh(III)	O, S	Octahedral	[29,30]
10	Ph	Alkyl	Alkyl	Au(I)	S	Linear	[31]
11	Fc	Py [f]	H	Fe(II)	O, N′, N″	Octahedral	This work

[a] The molecular structures (no. 1–10) have been elucidated by previous X-ray studies.
[b] Fc, ferrocenyl.
[c] Et, ethyl.
[d] Ph, phenyl.
[e] Naph, naphthyl.
[f] Py, pyridyl.

intense absorbances at ca. 469 (band I), ca. 387 (II) and ca. 348 nm (III), which are the characteristic absorption bands of ferrocene derivatives [32] and have been attributed to metal–ring charge transfer [33]. During irradiation with visible light, the bands I and II shift to lower energy from 469 to 502 nm and 387 to 398 nm (Fig. 3(b)). These spectral changes observed are indicative of a clean photochemical reaction giving rise to a single visible region absorbing product; no new absorption bands are observed in this region. Fortunately, the photoproduct can be isolated as a single crystal from the irradiated CH_3CN solution of HFT–py. The UV-vis absorption spectral changes are consistent with the results of crystal structure and provide further information concerning the photochemical reactions of HFT–py in CH_3CN solution.

3.4. Infrared spectroscopy

The main vibrational bands of HFT–py and [Fe(FT–py)$_2$] are listed in Table 7 for comparison. The IR spectra of HFT–py show a broad absorption between 3300 and 3100 cm^{-1} with a maximum at 3200 cm^{-1}, assignable to the stretching vibrations of the NH groups ν(NH) and pyridine ring ν(CH). The displacements to higher wavenumbers illustrate the participation of pyridine and imine nitrogen atoms in the coordination [15]. The strong stretch at 1660 cm^{-1}, assigned to the carbonyl stretch of the –C(O)–NH– moiety in uncomplexed ligand, is present at 1680 cm^{-1} for the complex. The coordinated pyridine ring can be distinguished from free one by the coupled ν(C=C) and

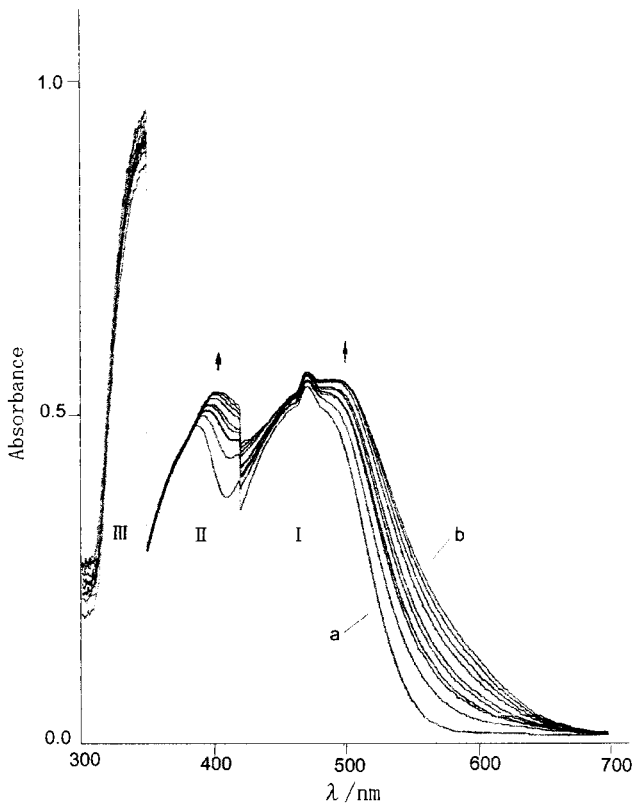

Fig. 3. Variation of the UV–vis spectra of HFT–py in degassed CH_3CN solution upon irradiation with visible light at 0°C, total HFT–py concentration, 2.25 mmol dm^{-3}. Curve a is the initial solution and curve b is for 1.5 h exposure. The spectra were recorded at 4–20 min intervals.

Table 7
Selected vibrational bond (cm^{-1}) of HFT–py and [Fe(FT–py)$_2$]

	$\nu_{(NH)}+\nu_{(CH)}$	$\nu_{(C=O)}$	py $\nu_{(C-N)}+\nu_{(C=C)}$	$\nu_{(N-C=S)}$	$\nu_{(C=S)}$	$\nu_{(C=S)}+\nu_{(N-C-N)}$
HFT–py	3200(br)	1660	1580	1430–1495	1294	1160, 820
Fe(FT–py)$_2$]	3500	1680	1600	1460–1540	1300	1160,820

ν(C=N) vibration from 1580 to 1600 cm^{-1} [16]. The bands at 1495–1430 cm^{-1} assigned to ν(–N–C=S) vibration [17] for the free ligand are displaced to 1540–1460 cm^{-1} for the complex. The medium band at ca. 1300 cm^{-1} is supposed to be ν(C=S) as reported before [18]. The vibrational bands at 1160 and 820 cm^{-1} in the spectra of the ligand may be attributed to the ν(N–C–S) stretching mode, or to a ν(C=S) and ν(N–C–N) coupling [19], which do not shift in the IR spectra of the complex, indicating that the thione group does not participate in the coordination. Therefore, the data mentioned above show that each ligand coordination in a tridentate manner via the pyridine and thioamidic nitrogen, and carbonyl oxygen atoms in good agreement with the structural results.

3.5. Mechanistic consideration

According to the mechanism proposed previously [2] and the results in this work, the photochemical reactions of HFT–py probably involve three steps (Scheme 1): the first is the photo-induced charge transfer from metal to carbonyl group, resulting in the deligation of HFT–py to free iron(II) ion, deprotonated *N*-cyclopentadienecarbonyl-*N*′-(2-pyridyl)thiourea anion (CT–py$^-$), and the unbonded cyclopentadienyl ring (Cp$^-$) (Eq.(1)). The second process is the proton-transfer from HFT–py to CT–py$^-$ and Cp$^-$, yielding FT–py$^-$ anion, HCT–py and 1,3-cyclopentadiene (Eqs.(2) and (3)). Apparently, the proton affinity of CT–py$^-$ and Cp$^-$ may be larger than HFT–py, this would be favorable to the proton-transfer process, and the third process is the formation of the complex between iron(II) cation and FT–py$^-$ anion. (Eq.(4))

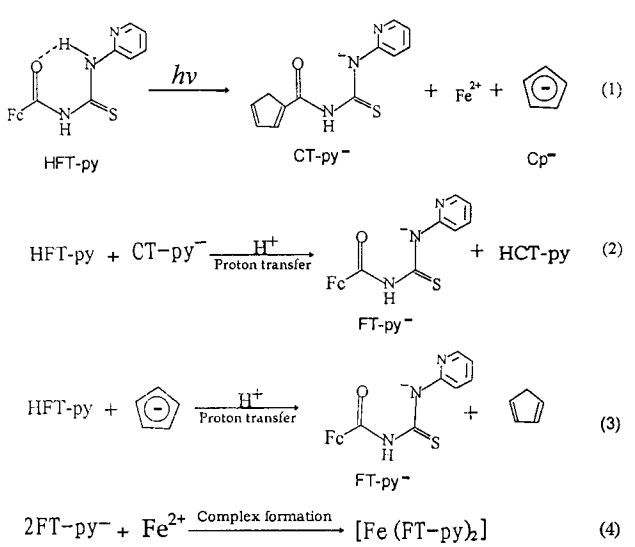

Scheme 1. Probable photo-reaction pathways.

4. Conclusions

The results of this work clearly illustrate that HFT–py as a ferrocenoyl-functionized thiourea ligand displays good photochemical behaviour, yielding a novel(O, N′, N″) coordinated iron(II) complex [Fe(FT–py)$_2$], which is apparently different from the coordination mode as in conventional *N*-acylthiourea coordination compounds and not available by usual thermochemical method. Therefore, further studies on such photoactive ligand system may be of interest in organometallic photochemistry and photosensitive materials.

5. Supplementary material

A complete table of crystallographic data, bond distances, bond angles, dihedral angles, atomic positional and thermal parameters, IR spectra of HFT–py and [Fe(FT–py)$_2$], as well as ^{1}H-NMR spectra of [Fe(FT–py)$_2$] are available from the authors.

Acknowledgements

We thank the Henan Science and Technology Committee for the financial support.

References

[1] D.J. Che, G. Li, B.S. Du, Z. Zhang, Y.H. Li, Inorg. Chim. Acta 261 (1997) 121.
[2] D.J. Che, G. Li, X.L. Yao, D.P. Zou, J. Organomet. Chem. 568 (1998) 165.
[3] A.M. Tarr, D.M. Wiles, Can. J. Chem. 46 (1968) 2725.
[4] E.K. Heaney, S.R. Logan, Inorg. Chim. Acta 22 (1977) L3.

[5] A. Togni, T. Hayashi (Eds.), Ferrocenes: Homogeneous Catalysis, Organic Synthesis, Material Science, VCH, Weinheim, 1995.
[6] (a) E.C. Constable, Angew. Chem. Int. Ed. Engl. 30 (1991) 407. (b) R.W. Wagner, P.A. Brown, T.E. Johnson, J. Chem. Soc. Chem. Commun. (1991) 1463. (c) P.D. Beer, Z. Chem, M.G.B. Brew, Inorg. Chim. Acta, 225 (1994) 137.
[7] M.C.B. Colbert, A.J. Edwards, J. Lewis, J. Chem. Soc. Dalton Trans. (1994) 2589.
[8] (a) J.S. Miller, A.J. Epstein, W.M. Reift, Chem. Rev. 88 (1988) 201. (b) J.S. Miller, A.J. Epstein, Angew. Chem. Int. Ed. Engl. 33 (1994) 385.
[9] M.M. Baizer, Organic Electrochemistry, Marcel Dekker, New York, 1973.
[10] Y.F. Yuan, L.Y. Zhang, J.P. Cheng, J.T. Wang, Trans. Met. Chem. 22 (1997) 281.
[11] TeXsan, Crystal Structure Analysis Package, Molecular Structure Corporation, 1985 and 1992.
[12] J.T. Wang, Y.F. Yuan, Y.M. Wu, J. Organomet. Chem. 481 (1994) 211.
[13] Y.F. Yuan, S.M. Ye, L.Y. Zhang, B. Wang, Inorg. Chim. Acta 256 (1997) 313.
[14] E.W. Ainscough, A.M. Brodie, Coord. Chem. Rev. 27 (1978) 59.
[15] L.J. Bellamy, Advances in Infrared Group Frequencies, Chapman and Hall, London, 1975.
[16] R. Bastida, A. DeBlas, D.E. Fenton, T. Rodriguez, Inorg. Chim. Acta 206 (1993) 47.
[17] C.N.R. Rao, R. Vankataroghavan, Spectrochem. Acta 18 (1962) 541.
[18] J.T. Wang, Chem. J. Chin. Univ. 16 (1995) 1415.
[19] J. Garcia-Tojal, J. Garcia-Jaca, R. Cortes, Inorg. Chim. Acta 249 (1996) 25.
[20] O. Seidelmann, L. Beyer, R. Richter, Z. Naturforsch. 50b (1995) 1679.
[21] P. Knuuttila, Acta Chim. Scand. A 36 (1982) 541.
[22] G.Z. Fitzl, Anorg. Allg. Chem. 433 (1977) 237.
[23] A. Irving, K.R. Koch, M. Matoetoe, Inorg. Chim. Acta 206 (1993) 193.
[24] R.A. Bailey, K.L. Rothaupt, Inorg. Chim. Acta 147 (1988) 233.
[25] S. Bourne, K.R. Koch, J. Chem. Soc. Dalton Trans. (1993) 2071.
[26] K.R. Koch, J.D. Toit, M.R. Caira, J. Chem. Soc. Dalton Trans. (1994) 785.
[27] V.R. Richter, L. Boyer, J. Kaiser, Z. Anorg. Allg. Chem. 461 (1980) 67.
[28] U. Braum, R. Richter, J. Sieler, Z. Anorg. Allg. Chem. 201 (1985) 526.
[29] J. Sieler, R. Richter, E. Hoyer, L. Beyer, Z. Anorg. Allg. Chem. 580 (1990) 167.
[30] W. Bensch, M. Schuster, Z. Anorg. Allg. Chem. 615 (1992) 93.
[31] W. Bensch, M. Schuster, Z. Anorg. Allg. Chem. 611 (1992) 99.
[32] A.M. Tarr, D.M. Willes, Can. J. Chem. 46 (1968) 2725.
[33] M. Rosenblum, Chemistry of the Iron Group Metallocenes, Interscience, New York, 1965, p. 42.